Q Structure of the Oceanic Crust

W. W. WEPFER and N. I. CHRISTENSEN

Department of Earth and Atmospheric Sciences, Purdue Rock Physics Laboratory, Purdue University, West Lafayette, IN 47907, U.S.A.

(Received 29 September, 1989; accepted 6 September, 1990)

Key words: Q, attenuation, ophiolite, oceanic crust, velocity.

Abstract. Compressional wave attenuations and velocities have been measured as a function of confining pressure in ophiolite samples representing a cross-section of the oceanic crust and uppermost mantle. Data are presented for basalts, diabase dikes, gabbros and a suite of serpentinites and peridotites showing a range of serpentization. An ultrasonic pulse-echo spectral ratio technique was used to determine the attenuations to confining pressures of 500 MPa. From this data a Q profile for the oceanic crust and upper mantle is presented. Q is found to moderately increase with depth through the pillow basalts of the upper oceanic crust. The sheeted dike rocks of Layer 2C show an increase in Q with depth due to progressive metamorphism (from greenschist to amphibolite facies). Q drops abruptly from Layer 2C to Layer 3, though it is not clear why the gabbros have such low Q's. The crust-mantle boundary is a Q discontinuity; however, the Q contrast between Layer 3 and the upper mantle could be altered by upper mantle serpentinization, interlayered gabbros and peridotites at the boundary, or serpentinized peridotite diapirs intruding the gabbroic section. Q varies significantly with the percentage of serpentinization in the ultramafic samples, with the largest changes in Q being at the extremes of zero and full serpentinization. Q is sensitive to the overburden pressure for all of the samples.

Introduction

The lithology and tectonics of the ocean crust are subjects of prime geologic importance which have consumed the efforts of many researchers over the last quarter century. Although ocean drilling has added to our knowledge, most of the direct data on oceanic crustal structure has come from marine seismic surveys. Following the summary of Raitt (1963), refraction investigations have provided detailed oceanic crustal layer thicknesses and velocities in many localities. Later work has expanded significantly on Raitt's three layer model, with velocity gradients and inversions commonly being found (e.g., Kempner and Gettrust, 1982).

Our understanding of the seismic structure of the ocean crust has been enhanced by studies of ophiolites. Ophiolites are generally acknowledged as being onland exposures of the ocean crust (Coleman, 1977), and laboratory physical properties studies of ophiolites have provided velocities as a function of depth through the crust with far more resolution than is available with current field methods. Complete compressional (V_p) and shear (V_s) wave velocity profiles have been constructed for the ocean crust and upper mantle from ophiolite traverses and seismic velocity variations have been correlated to ophiolite petrology (e.g., Salisbury and Christensen, 1978; Christensen and Smewing, 1981).

Although the variety structure of the ocean crust and upper mantle has been extensively explored, one seismic aspect has received little attention; the Q structure of the ocean crust. The seismic quality factor Q is inversely related to attenuation, i.e., a low Q means a high attenuation. Q data have been used to determine the location of subducting slabs (e.g., Oliver and Isacks, 1967; Bowman, 1988), but this type of work emphasizes variations in Q with temperature at a convergent margin. We are unaware of any field or laboratory work that constructs even a simple Q model for the ocean crust. This study seeks to develop a preliminary compressional wave Q (Q_p) profile based on laboratory data obtained on samples from the Red Mountain (New Zealand), Bay of Islands (Newfoundland), and Samail (Oman) ophiolites.

A Q model with depth from the oceanic crust is important because seismic amplitudes and arrival times oftentimes cannot be interpreted when velocities alone are considered (e.g., Orcutt *et al.*, 1975). In addition, Q is more sensitive to physical state variations than velocities (e.g., Born, 1941; Gardner *et al.*, 1964; Frisillo and Stewart, 1980; Clark *et al.*, 1980). This is particularly significant when using Q

data to invert for temperature variations, since changes in parameters such as alteration and state of saturation may also produce low Q's which could be confused with a high heat flow region. It is therefore apparent than an initial Q profile of the oceanic crust and upper mantle is needed before deviations from the norm can be examined.

Method

Applying confining pressure to a sample when determining its properties is important both for velocities and Q's (Birch and Bancroft, 1938a, b; Born, 1941; Birch, 1960, 1961). Pressure simulates *in situ* conditions and shows the effect of crack closure in raising Q's and velocities. Another consideration is sample size. Some laboratory techniques for measuring attenuation require long, thin rock samples (up to 2.5 cm in diameter and 100 cm in length [Murphy, 1982]) which can be difficult to obtain and prepare as well as being unwieldy in a pressure vessel. To avoid these problems, the pulse-echo spectral ratio technique of Winkler and Plona (1982) was employed, modified slightly to allow for the application of pressures to 500 MPa. The major modifications are the use of pressure insensitive damped transducers which have tungsten-epoxy backing pieces and the use of different buffer materials because of rock type and signal-to-noise (S/N) considerations. Figure 1 shows the sample assembly that is inserted into a pressure vessel capable of confining pressures in excess of 500 MPa.

In this method, a 1 MHz transducer converts an electrical input pulse to a transmitted seismic wave. This same transducer then receives the subsequent reflections. The reflection from the brass-sample interface is the first waveform to arrive. It has traveled only through the brass, which is considered non-attenuating relative to the rock and is thus the reference signal. The spectrum of this arrival gives the estimated source spectrum. The second waveform to arrive has reflected from the sample-steel interface and contains the desired attenuation information. Figure 2 shows these two arrivals, which are easily windowed (rectangular, tapered corners) and Fourier transformed to give the estimated spectra also shown in Figure 2. The spectra are corrected for diffraction effects according to the outline given in Winkler and Plona (1982). The attenuation coefficient α in dB/length is then determined from

$$\alpha(\omega) = \frac{8.686}{2L} \ln\left[\left|\frac{R_{23}}{R_{12}}\frac{A(\omega)}{B(\omega)}\right|(1 - R_{12}^2)\right]$$

(Winkler and Plona, 1982), where L is the sample

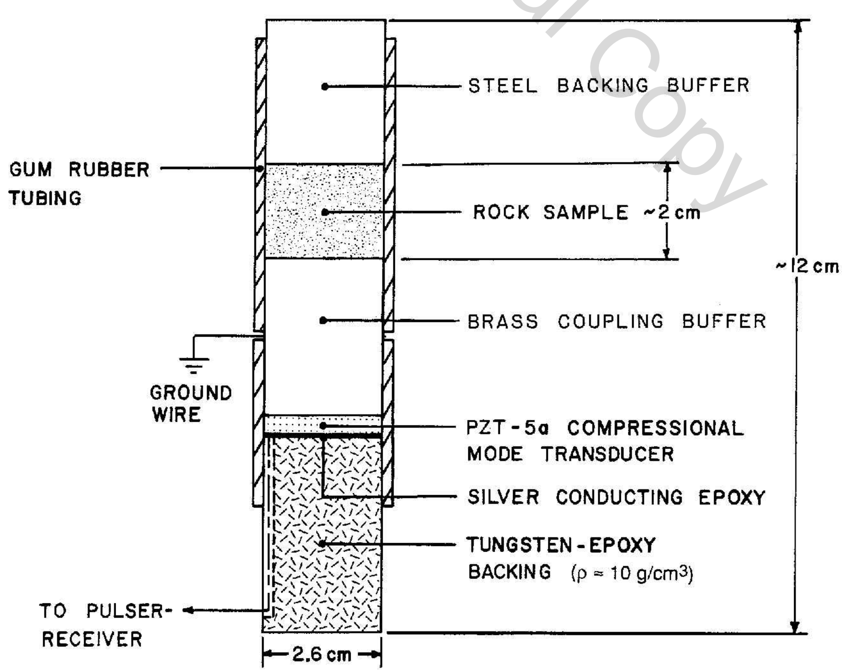

Fig. 1. Ultrasonic pulse-echo sample assumbly for determining P-wave attenuations to 500 MPa confining pressure.

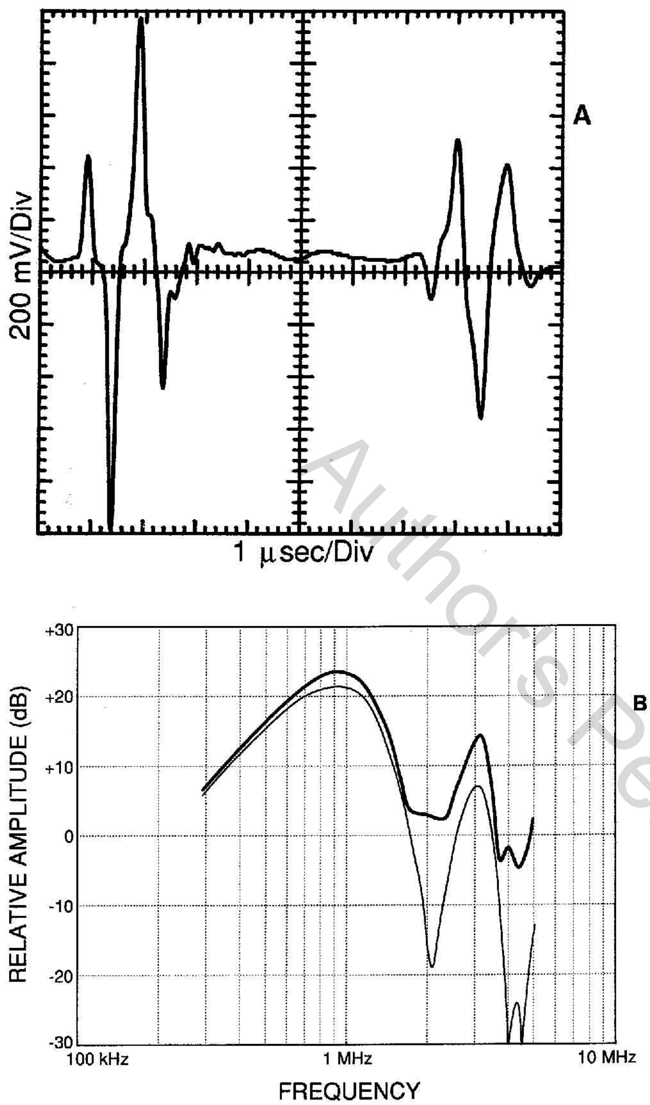

Fig. 2. (A) Reference and attenuated reflections from sample OMAN-37. (B) Spectra of the first (heavy line) and second waveforms.

length, A and B are the amplitude spectra of the first and second reflections, respectively, and the R's are the reflection coefficients with subscripts 1-2-3 corresponding to the brass-sample-steel assembly. As with most pulse techniques, the attenuation coefficient is measured and Q is derived using the equation

$$\frac{1}{Q}=\frac{\alpha V}{\pi f}$$

(Johnson and Toksoz, 1981), where V is the phase velocity, f is the frequency and α is in 1/length.

The accuracy of the pulse-echo technique has been checked using both high and low Q_p samples. Following the lead of Toksoz *et al.* (1979), an aluminum sample was used as a high Q_p reference. Aluminum is an excellent reference material because its compressional velocity and density are both similar to the rocks under consideration herein, as well as having a Q_p of over 10 000 (Zemanek and Rudnick, 1961). The measured attenuation of aluminum should therefore be 0.0 dB cm^{-1} at all pressures. Over the pressure range of 0 to 500 MPa, the attenuation coefficient was found to be (-0.02 ± 0.02) dB cm^{-1} for aluminum (Wepfer and Christensen, 1990). For low Q's, Berea sandstone is a good reference because it has been studied by many researchers. Unfortunately the Berea is also highly variable in mineralogy, with clearly visible differences from sample to sample, so the data should be judged accordingly. The value of $1000/Q_p$ for air dry Berea sandstone was found to range from 28 to 10 MPa to 12 at 200 MPa, results which compare favorably with the data of others (e.g., Johnston and Toksoz, 1980; Winkler, 1983, 1985). We conclude that the accuracy of this technique is about ± 0.05 dB cm^{-1} and may be slightly poorer for low Q rocks because of the associated low S/N ratios.

Sample preparation entails coring, trimming and polishing right circular cylinders of rock, typically 2.5 cm in diameter and 1.5 to 2 cm in length, which have flat and parallel faces to within ± 0.0005 cm. A copper foil jacket is placed around the sample to protect it from the high pressure oil. Compressional velocities as a function of confining pressure are measured first using the technique of Birch (1960) and described more fully by Christensen (1985). These group velocities (V_g) are used in determining the reflection coefficients in the attenuation coefficient equation. They are also used instead of the phase velocity in calculating $1/Q$ from α because V_g differs little from $V(f)$ at 1 MHz and the V_g measurements are substantially more accurate. Plots of $(V_p)_g$ versus pressure for ophiolite rocks are given in Christensen and Smewing (1981), Salisbury and Christensen (1978), and Christensen and Salisbury (1982). After the velocities have been measured, attenuations as a function of confining pressure are determined to 500 MPa.

Results

For this study, a selection of samples from the Bay of Islands, Newfoundland and Samail, Oman

TABLE I

Sample descriptions and petrography

Sample description	Petrography & Density (ρ)
BOI-152 Pillow Basalt	Intersertal, amygdalogidal. 40% plagioclase, 35% chlorite replacing glass, 20% calcite amygdule filling, 5% sphene. $\rho = 2.66 \times 10^3$ kg m^{-3}.
BOI-208 Basalt	Intergranular. 43% plagioclase, 40% clinoclinopyroxene, 10% chlorite, 3% sphene, 2% opaque, 2% carbonate. $\rho = 2.82 \times 10^3$ kg m^{-3}.
OMAN-9 Basalt	Intergranular, seriate. 45% plagioclase, 43% clinopyroxene, 7% chlorite, 5% opaque. $\rho = 2.72 \times 10^3$ kg m^{-3}.
OMAN-17 Metadiabase	Subophitic. 55% plagioclase, 20% chlorite, 19% pyroxene, 4% opaque, 2% carbonate. $\rho = 2.76 \times 10^3$ kg m^{-3}.
OMAN-14 Metadiabase	Subophitic. 55% plagioclase, 29% pyroxene, 20% chlorite, 5% opaque, 1% sphene. $\rho = 2.82 \times 10^3$ kg m^{-3}.
BOI-213 Metadiabase	Subophitic. 44% altered plagioclase, 28% hornblende, 20% actinolite, 4% orthopyroxene, 3% opaque, 1% prehnite. $\rho = 2.87 \times 10^3$ kg m^{-3}.
BOI-165 Metadiabase	Holocrystalline, inequigranular. 50% hornblende, 46% plagioclase, 2% epidote, 2% opaque. $\rho = 2.94 \times 10^3$ kg m^{-3}.
OMAN-23 Hornblende Gabbro	Intergranular high level gabbro. 45% plagioclase, 25% hornblende, 15% clinopyroxene, 8% chlorite, 5% actinolite, 2% opaque. $\rho = 2.90 \times 10^3$ kg m^{-3}.
BOI-167 Olivine Gabbro	Holocrystalline, inequigranular. 45% plagioclase, 30% clinopyroxene, 15% olivine, 6% amphibole, 3% chlorite, 1% opaque. $\rho = 2.90 \times 10^3$ kg m^{-3}.
OMAN-37 Gabbro	Equigranular. 40% plagioclase, 40% clinopyroxene, 10% orthopyroxene, 5% actinolite, 4% chlorite, 1% opaque. $\rho = 2.88 \times 10^3$ kg m^{-3}.
BOI-127 Olivine Gabbro	Holocrystalline, inequigranular, recrystallization patches, 37% plagioclase, 20% clinopyroxene, 15% olivine, 10% actinolite, 10% chlorite, 5% hornblende, 2% prehnite, 1% opaque. $\rho = 2.87 \times 10^3$ kg m^{-3}.
MAR-AII Serpentinite	Mesh structure. 91% serpentine, 5% olivine, 4% opaque. $\rho = 2.57 \times 10^3$ kg m^{-3}.
CYPRESS-624 Partially Serpentinized Peridotite	Mesh structure. 58% serpentine, 35% olivine, 5% orthopyroxene, 2% opaque. $\rho = 2.74 \times 10^3$ kg m^{-3}.
OMAN-52 Partially Serpentinized Peridotite	Equigranular, mesh structure. 46% serpentine, 45% olivine, 4% opaque, 5% orthopyroxene. $\rho = 2.84 \times 10^3$ kg m^{-3}.
CYPRESS-629 Partially Serpentinized Peridotite	Equigranular. 70% olivine, 15% orthopyroxene, 12% serpentine, 3% opaque. $\rho = 3.16 \times 10^3$ kg m^{-3}.
NZ-65 Harzburgite	Granular. 82% olivine, 15% orthopyroxene, 3% opaque. $\rho = 3.31 \times 10^3$ kg m^{-3}.

ophiolites were chosen, as well as peridotites from various locations showing a range of serpentinization. The samples were carefully selected to avoid the effects of scattering due to large grain sizes. This was accomplished by examining each sample in thin section and applying the average grain size scattering criterion of Mason *et al.* (1978). The petrographies for the samples are given in Table I. These rocks can be subdivided into the following four groups: (1) pillow basalts, representing oceanic Layers 2A and B; (2) sheeted dikes, representing Layer 2C; (3) gabbros, representing Layer 3; and (4) peridotites, representing the upper mantle and crustal diapiric intrusions. Figure 3 gives $1/Q$ as a function of confining pressure for one sample from each group, and Table II presents the Q_p and V_p data for all of the samples at selected pressures. All of the data are reported at a frequency of 1 MHz.

It is clear from Figure 3 and Table II that confining pressure has a significant effect on the observed Q values. As with velocities, this is due to the influence of cracks (Birch and Bancroft, 1938a, b). The *in situ* pressure is therefore an important consideration when discussing Q_p in the oceanic crust. Another factor is the effect of saturation. All of the data reported in Table II are air dry values. The

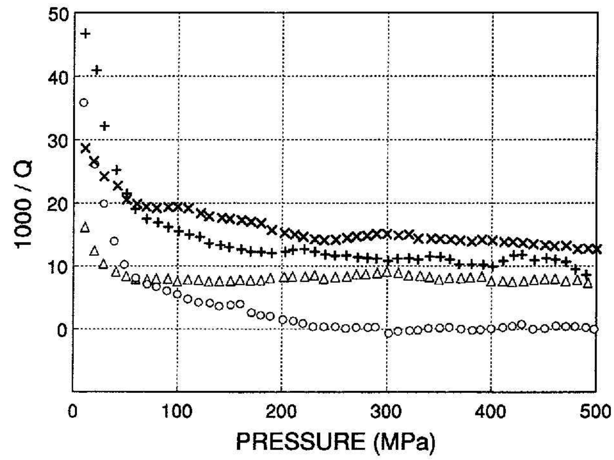

Fig. 3. $1000/Q_p$ for one sample from each group: OMAN-9 basalt (triangle), BOI-165 diabase (circle), BOI-127 gabbro (X), OMAN-52 serpentinized peridotite (plus).

TABLE II

Densities, compressional wave velocities (V_p) and attenuations (Q_p) at selected pressures for ophiolite samples, serpentinites and peridotites

Rock	Density ($g\ cm^{-3}$)	Confining pressure (MPa)					Confining pressure (MPa)				
		50	100	200 V_p($km\ s^{-1}$)	300	400	50	100	200 Q_p	300	400
Basalts											
BOI-152	2.66	5.41	5.58	5.76	5.87	5.95	55	62	76	116	145
BOI-208	2.82	5.27	5.47	5.65	5.76	5.84	79	83	108	159	295
OMAN-9	2.72	5.70	5.76	5.84	5.89	5.93	120	124	125	126	127
Diabases											
OMAN-17	2.76	5.89	6.03	6.16	6.23	6.29	52	72	73	85	104
OMAN-14	2.82	5.85	6.00	6.16	6.25	6.31	78	125	159	180	221
BOI-213	2.87	6.50	6.63	6.71	6.76	6.79	167	369	546	620	719
BOI-165	2.94	6.67	6.76	6.84	6.89	6.93	98	181	714	>900	>900
Gabbros											
OMAN-23	2.90	6.78	6.87	6.96	7.01	7.05	38	38	38	38	38
BOI-167	2.90	6.78	6.92	7.04	7.09	7.12	38	63	92	101	118
OMAN-37	2.88	6.77	6.85	6.93	6.98	7.01	33	35	37	39	41
BOI-127	2.87	6.98	7.03	7.10	7.12	7.14	47	53	66	69	72
Serpentinites and peridotites											
MAR-AII	2.57	4.41	4.54	4.71	4.83	4.92	13	14	14	16	23
CYP-624	2.74	5.52	5.59	5.68	5.75	5.80	66	71	73	82	97
OMAN-52	2.84	6.01	6.07	6.15	6.20	6.25	47	64	82	89	96
CYP-629	3.16	7.25	7.36	7.47	7.52	7.55	83	95	119	134	149
NZ-65	3.31	8.18	8.25	8.30	8.33	8.35	211	237	272	320	390

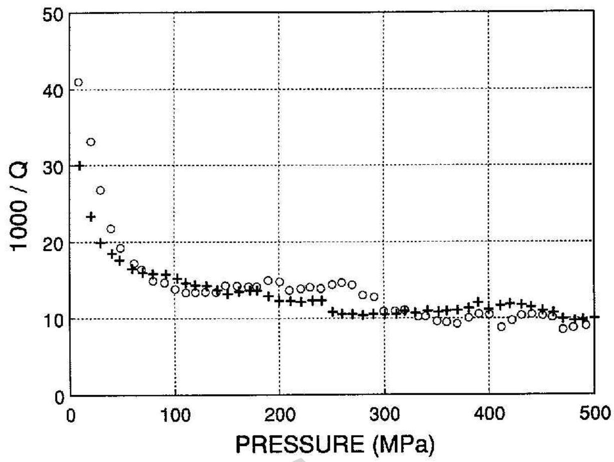

Fig. 4. Saturated (plus) and dry (circle) attenuation data for OMAN-17 metadiabase. Saturation has little effect on the Q's of this low porosity sample.

porosities are small (less than 1%) for all of the samples, so one would expect the influence of saturation to be minimal. This is verified in Figure 4, which shows that saturation changes the Q values relatively little (and well within the accuracy of the experiments) for a sheeted dike from the Oman ophiolite. The application of air dry Q data directly to the ocean crust therefore appears justified for these samples. In the uppermost basalt section, however, water saturation may lower Q (Wepfer and Christensen, 1990). Finally, Q anisotropy may be an important factor, though little experimental work has been done in this area. However, all of the rocks used in this study have a V_p anisotropy of less than 5 to 6%, so it is anticipated that any Q_p anisotropy is of similar magnitude.

Discussion

A simple Q_p model for the crystalline ocean crust is given in Figure 5. Also shown are the compressional velocities versus depth. The lithology profile is similar to that of Christensen and Smewing (1981) and Christensen and Salisbury (1982). The overburden pressure for each sample is calculated based on the estimated depth of burial and a 4 km water column; the Q_p and V_p data at these pressures are used in Figure 5. Sample depths are estimated from their stratigraphic locations.

Four distinct depth intervals are defined in Figure 5, and these are discussed below in terms of petrography, Q_p and V_p.

0–1 km: Pillow basalts

All three basalts have similar Q_p and V_p values. Both V_p and Q_p show increases with depth through the pillow basalt layer. These basalts have some alteration (Table I), and the sample with the highest alteration product content, BOI-152, also has the lowest Q's (Table II). Heavily altered near-surface basalts probably have lower Q's (Wepfer and Christensen, 1990).

Another consideration is the presence of fractures and rubble zones in the upper oceanic crust, the existence of which has been established by detailed seismic studies of Layer 2 (Houtz and Ewing, 1976). Laboratory specimens are too small to contain these large scale features, and hence laboratory velocities at low pressures are higher than those found both by refraction and logging studies (Hess, 1962; Hyndman and Drury, 1976; Kirkpatrick, 1979). However, laboratory velocities at higher pressures are in agreement with logging and refractive velocities at greater depths because these fractures are primarily closed or filled (Salisbury *et al.*, 1979). Laboratory velocities for Layers 2A and B thus represent upper bounds to that which would actually be determind in the field, a conclusion which should also hold for Q, i.e., significant fracturing is expected to reduce the observed Q's in the upper oceanic crust. This contention agrees with the oceanic field data of Jacobsen and Lewis (1988) who found Q's as low as 25 near the surface and an increase to 100 at 600 m depth.

1–3 km: Sheeted dikes

The two sheeted dike samples from the upper section of the Samail ophiolite are of greenschist facies (Figure 5). They have mineralogies, densities and Q's similar to the three basalts and slightly higher velocities (Tables I and II). The two sheeted dike rocks from the Bay of Islands ophiolite have undergone extensive recrystallization and contain abundant hornblende (Table I), thus putting them in the amphibolite facies (Figure 5). These two have much higher velocities, densities and Q's than the overlying samples (Table II). Progressive metamorphism from the greenschist to amphibolite facies therefore causes an increase in both Q_p and V_p with depth. These conclusions can be drawn with a good degree of

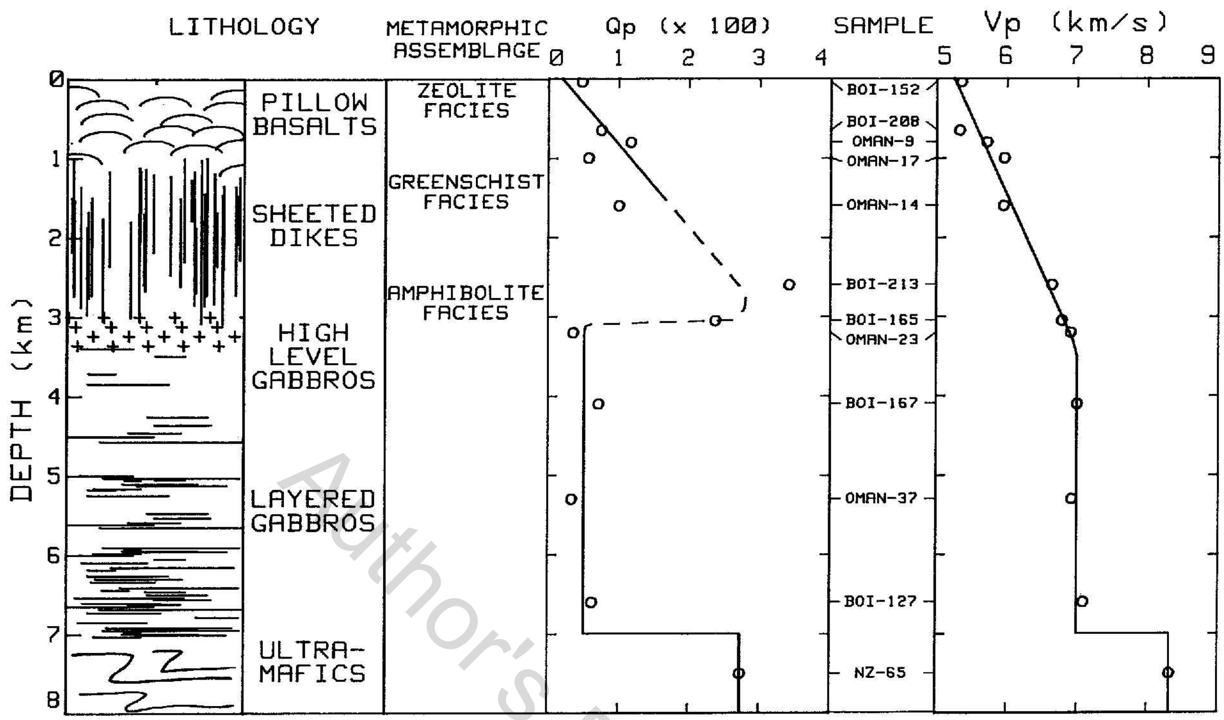

Fig. 5. Lithology, Q_p and V_p profiles for the oceanic crust. The data are at the appropriate overburden pressures and at a frequency of 1 MHz. The presence of large scale fracturing and other porosity in the upper crust will further lower Q's and velocities.

certainty because large scale fracturing is greatly diminished in Layer 2C (Salisbury *et al.*, 1979), meaning that laboratory and field data should compare favorably.

Although Q_p is definitely higher in the lower section of the sheeted dikes, the exact profile is not well constrained. Because of this, the curve in Figure 5 is dashed in this region. The first region for this is the lack of control with only two amphibolite facies dike samples. The second is that metamorphism is patchy at this depth due to the variability of hydrothermal circulation (Pallister, 1981). Hence these two samples probably give maximum Q's for this depth, and the exact profile depends on the extent of recrystallization in a given region.

The V_p-depth model for the first 3 km depth in Figure 5 is comparable to the profiles of Christensen and Smewing (1981) for the Samail ophiolite and Christensen and Salisbury (1982) from the Bay of Islands ophiolite. V_p increases from 5.5 to 7.0 km s^{-1}, an increase by a factor 1.25. In contrast, Q_p increases by about five to ten times from 0 to 3 km.

3–7 km: Gabbros

The most striking feature of the Q_p profile given in Figure 5 is the sharp decrease in Q at 3 km. Table II shows that the Q's for the four gabbros are consistently lower than any of the other three sample groups. It is not clear why this occurs. Petrologically gabbros are the coarse-grained equivalents of basalts, so mineralogical considerations shed no light. For example, basalt sample BOI-208 is compositionally almost identical to gabbro sample OMAN-37 and their densities are within 2% of each other (Table I), yet BOI-208 has a Q_p of nearly 300 at 400 MPa while OMAN-37 has a Q_p of 38 (Table II).

One possible explanation for the low Q's of the gabbros is that scattering occurs at 1 MHz because of their relatively large grain sizes. Three lines of evidence contradict this verdict. First, fine-grained samples were chosen throughout to avoid the effects of scattering. 'Fine-grained' is defined in terms of the typical grain size relative to the wavelength using the criterion of Mason *et al.* (1978); they state that the average grain size must be one-third the wavelength or greater for scattering to occur in rocks. All of the samples in this study exceed this requirement, having an average grain size at least one-sixth smaller than the wavelength at 1 MHz. Second, the specimens with the largest grains from the other three sample groups gave the highest Q's (BOI-208 for the basalts, BOI-213 for the dikes, NZ-65 for the peridotites). Also, Q decreases with decreasing grain size for the serpentinized peridotites. Third, the two gabbros with the smallest grain sizes, OMAN-23 and OMAN-37, have the lowest Q's. Hence an appeal to scattering does not give a reasonable explanation for the low Q behavior of the gabbros. Other explanations may revolve around some type of frequency dependent effects on Q. It is not at all obvious why such effects would apply only to the gabbros, however.

Other laboratory studies which determined Q's not only for gabbros but also for basalts, diabases and/or peridotites could provide support for the low Q's observed for the gabbros, since the relative values could then be compared with the results given in Figure 5. Volarovich and Gurvich (1957) measured Q_s for two basalts, one diabase and one gabbro in the frequency range of 3 to 4 kHz. At room pressures and temperatures Q_s for the diabase was about twice that of the basalts, while Q_s for the gabbro was less than one-half that of the basalts. This trend is similar to the Q_p profile given in Figure 5 (bearing in mind, of course, that Volarovich and Gurvich (1957) measured Q_s, not Q_p, at frequencies much below 1 MHz). In a subsequent study, Volarovich *et al.* (1960) measured Q_p at 1 MHz for a basalt, a gabbro and a gabbro-diorite under room conditions. The gabbro and gabbro-diorite had Q_p's 1.5 and 3.6 times less than that of the basalt, respectively. These results serve to bolster the conclusion that Q_p is low for gabbros, though no explanation for this behavior is evident.

The gabbros have slightly higher velocities and densities than the overlying dikes. Both the V_p- and Q_p-depth plots based on these samples show constant values for Layer 3, though the presence of such features as dikes, sills and diapirs would vary the profile in a given area. Sample OMAN-23 is a massive high level gabbro which has abundant hornblende (Table I). The three underlying gabbros contain abundant pyroxene (Table I). The two olivine-bearing gabbros (BOI-167 and BOI-127) have slightly higher Q's than the other two gabbros (Table II).

Below 7 km: Peridotites

The boundary between the layered gabbros of Layer 3 and the underlying peridotites is the seismic Moho. The peridotites found in ophiolites usually have a large serpentine content, but the serpentinization likely represents post-emplacement alteration (Wenner and Taylor, 1973; Coleman, 1977). Based on the assumption that the oceanic upper mantle is unserpentinized, the profile in Figure 5 below the Moho is derived from the single data point for NZ-65, an extremely fresh (unserpentinized) tectonite (Table I). The density, velocity and Q of this harzburgite are all high (Table II).

Five ultramafic rocks have been studied, four of which are from ophiolite sequences. Two samples are from Cypress Island off the coast of the state of Washington. OMAN-52 is from the Samail, Oman ophiolite. The harzburgite NZ-65 is from the Red Hills, New Zealand ophiolite. MAR-AII is a Mid Atlantic Ridge sample dredged near St. Paul's Rocks. It is almost fully serpentinized. These rocks represent a range from zero to nearly full serpentinization. Christensen (1966) showed a linear relationship between V_p and density for peridotites, the density being indicative of the serpentine content. A similar relationship is shown in Figure 6 for the five

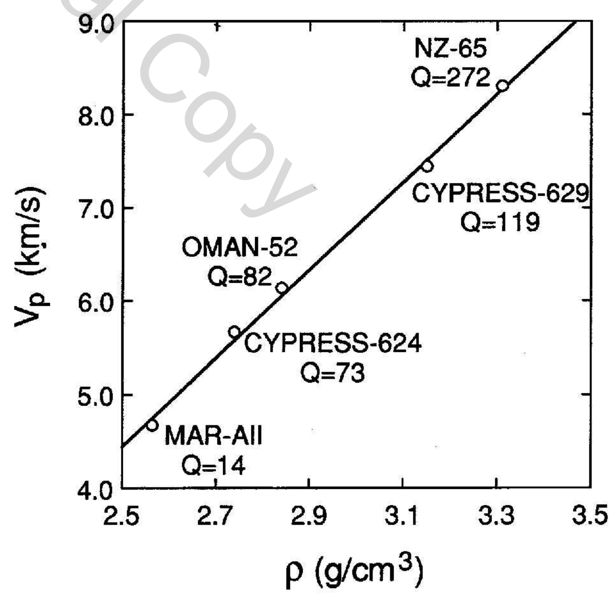

Fig. 6. Velocity-density plot for serpentinites and peridotites, with Q_p indicated. V_p and Q_p data are at a confining pressure of 200 MPa. Q_p is very sensitive to the serpentine content, especially at the extremes of full and zero serpentinization.

peridotites studied herein. Compressional velocities at 200 MPa are plotted as a function of density, giving the relationship

$$V_p(200\text{ MPa}) = 4.69\rho - 7.25$$

with a correlation coefficient of 0.998, where ρ is the density in g cm^{-3} and V_p is the velocity in km s^{-1}. Indicated beside each point is the Q_p value at 200 MPa. No simple relationship between Q_p and density has been found, but it appears that Q_p drops significantly upon initial serpentization and decreases gradually until nearly complete serpentinization reduces Q_p to very low values. Evidently, then, Q_p is more sensitive to the serpentine content than the corresponding velocities, especially at the density extremes. This relationship may be helpful in evaluating the percentage of serpentine in the lower oceanic crust, a subject which sparked considerable discussion in early oceanic work (Hess, 1962; Dietz, 1963; Cann, 1968) and is still controversial (e.g., Clague and Straley, 1977; Francis, 1981).

Any significant volume of serpentinization in the upper mantle would reduce the V_p and Q_p contrasts at the Moho, making the step in Figure 5 less sharp. Additionally, serpentine diapirs may be present in Layer 3 as suggested by Bonatti and Honnorez (1976). The volume of diapirs and their degree of serpentinization will determine their effect on Layer 3 Q. Upper mantle and lower crustal V_p will be uniformly reduced with increasing serpentinization (Figure 6), and Poisson's ratio will be high (Christensen, 1972). Thus the presence of serpentine diapirs in Layer 3 and upper mantle serpentinization could significantly alter the V_p and Q_p contrasts at the Moho.

Some regions of ophiolites show a transitional interface at the Moho, with interlayered gabbros and peridotites at the contact (Collins *et al.*, 1986). The proportion of peridotite layers relative to the gabbros increases with depth in such areas. This would give a steep V_p and Q_p gradient at the Moho rather than the step increase shown in Figure 5, assuming no signficant serpentinization of the peridotite layers.

Velocity anisotropy in peridotites can be significant, so Q anisotropy may likewise be an important consideration. The magnitude of the Q_p anisotropy for NZ-65 has not been determined, however, so it is not clear what effect Q anisotropy would have on the model in Figure 5 below the Moho. Petrofabric analysis and velocity anisotropy calculations were performed on NZ-65, and the results are given in Figure 7. Olivine fabric diagrams were obtained from universal stage measurements of 100 grains, and these are shown in Figure 7a–c. The preferred olivine orientation is quite strong for all three crystallographic axes. Using the computer program of Crosson and Lin (1971), which determines the contribution of each mineral to the rock's velocity in each direction, the V_p anisotropy was calculated at a confining pressure of 200 MPa. The velocity results are given in Figure 7d. The sample chosen for the Q measurements is one with an average velocity and its orientation is indicated by a plus sign in the figure. Presumably a sample with an average V_p would give an average Q_p for the rock as well, though this is based on the unverified assumption that velocities and Q's are influenced by the same factors. The 200 MPa velocity predicted from petrofabrics agrees well with the measured velocity for NZ-65 given in Table II.

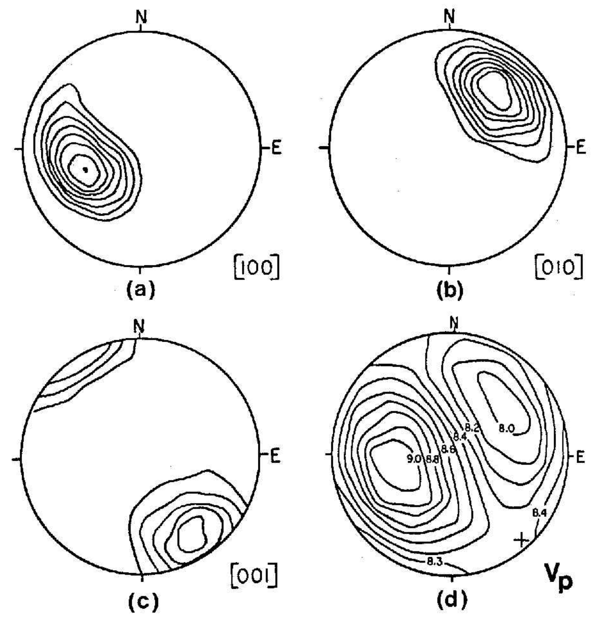

Fig. 7. Petrofabric analysis for harzburgite NZ-65 olivine crystals (a–c) and calculated V_p anisotropy (d). Q sample orientation given by plus sign in (d).

Frequency Dependence of Q

Q has generally been found to be frequency independent for dry rock (Johnston, 1981; Spencer, 1981). This has been a matter of much discussion, however.

If the attenuation mechanism in operation for these rocks gives a Q which is frequency independent, our results are directly applicable to the ocean crust. A number of attenuation mechanisms and phenomenological descriptions have been proposed which give a frequency independent Q (Futterman, 1962; Walsh, 1966; Savage, 1966; Kjartansson, 1979). If the mechanism is frequency dependent, the model in Figure 5 may yet be valid if the Q's are simply scaled according to the frequency range, e.g., if *all* Q's are lowered by a certain percentage at higher frequencies. Such a loss mechanism was proposed by Mason and coworkers (Mason, 1969; Mason and Kuo, 1971; Mason *et al.*, 1978). Both of these cases assume that the same mechanism is in operation throughout the frequency range, an assumption which may not be valid. Since no generally accepted attenuation mechanism exists, however, the conclusions expressed in our oceanic crustal Q_p model are strictly applicable only at 1 MHz.

Conclusions

Velocity-depth profiles derived from ophiolite studies have added to our knowledge of the seismic structure of the oceanic crust. Building on this foundation, a preliminary Q_p-depth model for the oceanic crust and upper mantle based on laboratory data obtained from ophiolite samples is presented. The Q_p profile (Figure 5) shows the following significant feature:

(1) Q_p increases with depth through the pillow basalts of oceanic Layers 2A and B. Near-surface fracturing and alteration should lower the Q's observed in the field.

(2) The sheeted dike interval (Layer 2C) shows increasing Q's with depth due to progressive metamorphism.

(3) Q_p is lowest in Layer 3, the gabbroic interval. This unexpected result should be a target of future marine seismic investigations.

(4) The Mohorovicic discontinuity represents a sharp contrast in Q_p between overlying layered gabbros and underlying peridotites. This contrast may be changed by serpentinization of the upper mantle, interlayered gabbros and peridotites at the crust-mantle boundary or serpentine diapirs intruding Layer 3.

Water saturation has little effect on the Q_p values of low porosity (less than 1%) oceanic rocks. Q_p is sensitive to the applied confining pressure, so the *in situ* pressures must be considered when making comparisons between laboratory and field Q data. Q_p is more sensitive to the percentage of serpentinization in peridotites than the associated compressional velocities, especially at the extremes of 0 and 100% serpentinization.

Acknowledgments

Our thanks to R. L. Nowack and L. W. Braile for their comments on this manuscript. Thanks also to A. Kulshrestha and M. Fagan for their help in constructing the transducers backing pieces. This research was supported by the Office of Naval Research under contracts N-00014-84-K-0207 and N-00014-89-J-1209 (N. I. Christensen) and by a Purdue David Ross fellowship (W. W. Wepfer).

References

Birch, F., 1960, The Velocity of Compressional Waves in Rocks to 10 Kilobars, Part 1, *J. Geophys. Res.* **65**, 1083–1102.

Birch, F., 1961, The Velocity of Compressional Waves in Rocks to 10 Kilobars, Part 2, *J. Geophys. Res.* **66**, 2199–2224.

Birch, F. and Bancroft, D., 1938a, The Effect of Pressure on the Rigidity of Rocks, I, *J. Geol.* **46**, 59–87.

Birch, F. and Bancroft, D., 1938b, The Effect of Pressure on the Rigidity of Rocks, II, *J. Geol.* **46**, 113–141.

Bonatti, E. and Honnorez, J., 1976. Sections of the Earth's Crust in the Equatorial Atlantic, *J. Geophys. Res.* **81**, 4104–4116.

Born, W. T., 1941, The Attenuation Constant of Earth Materials, *Geophysics* **6**, 132–148.

Bowman, J. R., 1988, Body Wave Attenuation in the Tonga Subduction Zone, *J. Geophys. Res.* **93**, 2125–2139.

Cann, J. R., 1968, Geological Processes at Mid-Ocean Ridge Crests, *Geophys. J. R. Astr. Soc.* **15**, 333–341.

Christensen, N. I., 1966, Elasticity of Ultrabasic Rocks. *J. Geophys. Res.* **71**, 5921–5931.

Christensen, N. I., 1972, The Abundance of Serpentinites in the Oceanic Crust, *J. Geol.* **80**, 709–719.

Christensen, N. I., 1985, Measurements of Dynamic Properties of Rock at Elevated Temperatures and Pressures, in Pincus, H. J. and Hoskins, E. R. (eds.), *Measurement of Rock Properties at Elevated Pressures and Temperatures*, ASTM STP 869, American Society for Testing and Materials, Philadelphia, 93–107.

Christensen, N. I. and Salisbury, M. H., 1982, Lateral Heterogeneity in the Seismic Structure of the Ocean Crust Inferred from Velocity Studies in the Bay of Islands, Ophiolite, Newfoundland, *Geophys. J. R. Astr. Soc.* **68**, 675–688.

Christensen, N. I. and Smewing, J. D., 1981, Geology and Seismic Structure of the Northern Section of the Oman Ophiolite, *J. Geophys. Res.* **86**, 2545–2555.

Clague, D. A. and Straley, P. F., 1977, Petrologic Nature of the Oceanic Moho, *Geology* **5**, 133–136.

Clark, V. A., Tittmann, B. R., and Spencer, T. W., 1980, Effect of Volatiles on Attenuation ($1/Q$) and Velocity in Sedimentary Rocks, *J. Geophys. Res.* **85**, 5190–5198.

Coleman, R. G., 1977, Ophiolites: Ancient Oceanic Lithosphere? Wyllie, P. J., von Engelhardt, W. and Hahn, T. (eds.), *Minerals and Rocks* **12**, Springer-Verlag, Germany.

Collins, J. A., Brocher, T. M., and Karson, J. A., 1986. Two-Dimensional Seismic Reflection Modeling of the Inferred Fossil Oceanic Crust/Mantle Transition in the Bay of Islands Ophiolite, *J. Geophys. Res.* **91**, 12520–12538.

Crosson, R. S. and Lin, J. W., 1971, Voight and Reuss Prediction of Anisotropic Elasticity of Dunite, *J. Geophys. Res.* **76**, 570–578.

Dietz, R. S., 1963, Alpine Serpentines as Oceanic Rind Fragments, *Bull. GSA* **74**, 947–952.

Francis, T. J. G., 1981, Serpentinization Faults and their Role in the Tectonics of Slow Spreading Ridges, *J. Geophys. Res.* **86**, 11616–11622.

Frisillo, A. L. and Stewart, T. J., 1980, Effect of Parital Gas/Brine Saturation on Ultrasonic Absorption in Sandstone, *J. Geophys. Res.* **85**, 5209–5211.

Futterman, W. I., 1962, Dispersive Body Waves, *J. Geophys. Res.* **67**, 5257–5291.

Gardner, G. H. F., Wyllie, M. P. J., and Droschak, D. M., 1964, Effects of Pressure and Fluid Saturation on the Attenuation of Elastic Waves in Sands, *J. Pet. Tech.* **16**, 189–198.

Hess, H. H., 1962, History of Ocean Basins, in Engel, A. E. J. (ed.), *Petrologic Studies*: A volume to honor A. F. Buddington, *Bull GSA*, 599–620.

Houtz, R. and Ewing, J., 1976, Upper Crustal Structure as a Function of Plate Age, *J. Geophys. Res.* **81**, 2490–2498.

Hyndman, R. D. and Drury, M. J., 1976. The Physical Properties of Oceanic Basement Rocks from Deep Sea Drilling on the Mid-Atlantic ridge, *J. Geophys. Res.* **81**, 4042–4059.

Jacobson, R. S. and Lewis, B. T. R., 1988, Attenuation Results from the Uppermost Young Oceanic Crust, *EOS*, *Trans. Am. Geophys. Un.* **69**, 406.

Johnston, D. H., 1981, Attenuation: A State-of-the-Art Summary, in Johnston, D. H. and Toksoz, M. N. (eds.), *Seismic Wave Attenuation*, SEG Geophys. Reprint Ser. No. 2, Tulsa, 123–135.

Johnston, D. H. and Toksoz, M. N., 1980, Ultrasonic P and S Wave Attenuation in Dry and Saturated Rocks under Pressure, *J. Geophys. Res.* **85**, 925–936.

Johnston, D. H. and Toksoz, M. N., 1981, Definitions and Terminology, in Johnston, D. H. and Toksoz, M. N. (eds.), *Seismic Wave Attenuation*, SEG Geophys. Reprint Ser. No. 2, Tulsa, 1–5.

Kempner, W. C. and Gettrust, J. F., 1982, Ophiolites, Synthetic Seismograms and Ocean Crustal Structure 1. Comparison of Ocean Bottom Seismometer Data and Synthetic Seismograms for the Bay of Islands Ophiolite, *J. Geophys. Res.* **87**, 8447–8462.

Kirkpatrick, R. J., 1979, The Physical State of the Oceanic Crust: Results of Downhole Geophysical Logging in the Mid-Atlantic Ridge at 23 °N, *J. Geophys. Res.* **84**, 178–188.

Kjartansson, E., 1979, Constant Q-Wave Propagation and Attenuation, *J. Geophys. Res.* **84**, 4737–4748.

Mason, W. P., 1969, Internal Friction Mechanism that Produces an Attenuation in the Earth's Crust Proportional to the Frequency, *J. Geophys. Res.* **74**, 4963–4966.

Mason, W. P. and Kuo, J. T., 1971, Internal Friction of Pennsylvania Slate, *J. Geophys. Res.* **76**, 2084–2089.

Mason, W. P., Marfurt, K. J., Beshers, D. N., and Kuo, J. T., 1978, Internal Friction in Rocks, *J. Acoust. Soc. Am.* **63**, 1596–1603.

Murphy, W. F., III, 1982, Effects of Partial Water Saturation on Attenuation in Massilon Sandstone and Vycor Porous Glass, *J. Acous. Soc. Am.* **71**, 1458–1468.

Oliver, J. and Isacks, B., 1967, Deep Earthquakes Zones, Anomalous Structures in the Upper Mantle, and the Lithosphere, *J. Geophys. Res.* **72**, 4259–4275.

Orcutt, J., Kennett, B., Dorman, L., and Prothero, W., 1975, Low Velocity Zone Underlying Fast-spreading Rise Crest, *Nature* **256**, 475–476.

Pallister, J. D., 1981, Structure of the Sheeted Dike Complex of the Samail Ophiolite near Ibra, Oman, *J. Geophys. Res.* **86**, 2661–2672.

Raitt, R. W., 1963, The Crustal Rock, in Hill, M. N. (ed.), *The Sea*, **3**, Interscience, New York, 85–102.

Salisbury, M. H. and Christensen, N. I., 1978, The seismic Velocity Structure of a Traverse Through the Bay of Islands Ophiolite Complex, Newfoundland, an Exposure of Oceanic Crust and Upper Mantle, *J. Geophys. Res.* **83**, 805–817.

Salisbury, M. H., Stephen, R., Christensen, N. I., Francheteau, J., Hammano, Y., Hobart M., and Johnson, D., 1979, The Physical State of the Upper Levels of Cretaceous Oceanic Crust from the Results of Logging, Laboratory Studies and the Oblique Seismic Experiment at DSDP sites 417 and 418, in *Deep Drill Results in the Atlantic Ocean: Ocean Crust*, Maurice Ewing Ser. 2, AGU, Washington, DC, 113–134.

Savage, J. C., 1966, Thermoelastic Attenuation of Seismic Waves by Cracks, *J. Geophys. Res.* **71**, 3929–3938.

Spencer, T. W., Jr., 1981, Stress Relaxations at Low Frequencies in Fluid-Saturated Rocks: Attenuation and Modulus Dispersion, *J. Geophys. Res.* **86**, 1803–1812.

Toksoz, M. N., Johnston, D. H., and Timer, A., 1979, Attenuation of Seismic Waves in Dry and Saturated Rocks, I, Laboratory Measurements, *Geophysics* **44**, 681–690.

Volarovich, M. P. and Gurvich, A. S., 1957, Investigation of Dynamic Moduli of Elasticity for Rocks in Relation to Temperature, *Bull. (Izv.) Acad. Sci. USSR, Geophys. Ser.* **4**, 1–9.

Volarovich, M. P., Levykin, A. I., and Sizov, V. P., 1960, Investigation of the Attenuation of Elastic Waves in Rock Specimens, *Bull. (Izv.) Acad. Sci. USSR, Geophys. Ser.* **8**, 793–797.

Walsh, J. B., 1966, Seismic Wave Attenuation in Rock Due to Friction, *J. Geophys. Res.* **71**, 2591–2599.

Wenner, D. B. and Taylor, Jr., H. P., 1973, Oxygen and Hydrogen Isotope Studies of the Serpentinization of Ultramafic Rocks in Oceanic Environments and Continental Ophiolite Complexes, *Am. J. Sci.* **273**, 207–239.

Wepfer, W. W. and Christensen, N. I., 1990, Compressional Wave Attenuation in Oceanic Basalts, *J. Geophys. Res.* **95**, 17431–17439.

Winkler, K. W., 1983, Frequency Dependent Ultrasonic Properties of High-Porosity Sandstones, *J. Geophys. Res.* **88**, 9493–9499.

Winkler, K. W., 1985, Dispersion Analysis of Velocity and Attenuation in Berea Sandstone, *J. Geophys. Res.* **90**, 6793–6800.

Winkler, K. W. and Plona, T. J., 1982, Technique for Measuring Ultrasonic Velocity and Attenuation Spectra in Rocks Under Pressure, *J. Geophys. Res.* **87**, 10776–10780.

Zemanek, J. and Rudnick, I., 1961, Attenuation and Dispersion of Elastic Waves in a Cylindrical Bar, *J. Acoust. Soc. Am.* **33**, 1283–1288.